JOC The Journal of Organic Chemistry

Article

Cite This: J. Org. Chem. 2019, 84, 14805−14815

pubs.acs.org/joc

How Resonance Modulates Multiple Hydrogen Bonding in Self-Assembled Systems

Xuhui Lin,[†] Wei Wu,[†] and Yirong Mo*[,‡]

[†]The State Key Laboratory of Physical Chemistry of Solid Surfaces, iChEM, Fujian Provincial Key Laboratory of Theoretical and Computational Chemistry and College of Chemistry and Chemical Engineering, Xiamen University, Xiamen, Fujian 361005, China

[‡]Department of Chemistry, Western Michigan University, Kalamazoo, Michigan 49008, United States

Supporting Information

ABSTRACT: The secondary electrostatic interaction (SEI) has been regarded as the fundamental cause for the relative strengths of multiple hydrogen bonds for decades, though recent studies challenged its validation. Here, we used our developed block-localized wave function (BLW) method, which is a variant of ab initio valence bond (VB) theory and can self-consistently derive the wave function for a strictly electron-localized state, to study a series of exemplary multiply hydrogen-bonded complexes and critically examine the role of SEI in the binding. Our computations show that the multiple hydrogen bond in self-assembled complexes is a kind of resonance-assisted hydrogen bond (RAHB) in nature, and the π resonance which moves electron density from the hydrogen bond donor to the acceptor is the true origin of the different hydrogen bond strengths. By quenching the π resonance effect, the hydrogen bond strengths become nearly identical for various neutral doubly, triply, and quadruply hydrogen-bonded dimers where in general the SEI model works. In other words, the SEI plays only a minor role in multiply hydrogen-bonded complexes, and the π resonance, which changes not only electron densities but also molecular polarities (dipole moments), is the major force.

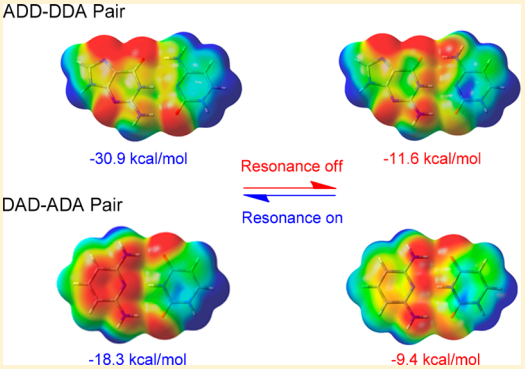

1. INTRODUCTION

Supramolecular chemistry has emerged as an active and productive multidisciplinary research domain which focuses on the rational design and development of functional complex architectures by putting multiple chemical components together through noncovalent interactions.[1−3] It has been extensively explored and applied in broad areas such as drug development,[4,5] molecular devices,[6] sensors,[7,8] catalysis,[9,10] nanoscience,[11] and material science.[12−14] The structures and properties of supramolecular systems are governed by noncovalent interactions[1,2,15] which, based on the nature of the particular components directly involved in the interactions, include Coulombic (electrostatic) interactions, hydrogen bonding, charge transfer, van der Waals (dispersion), and recently identified halogen bonding,[16−18] chalcogen bonding,[19,20] pnicogen bonding,[21] tetrel bonding,[22] π-ion,[23,24] π/π stacking,[25,26] and so on. In chemical components usually there are multiple binding sites which not only change the overall binding strength but also allow the manipulation of complex structures by modulating the binding sites. In general, however, the interactions in multiple binding sites may be cooperative or anticooperative, leading to mutual either strengthening or weakening of the overall binding.[27] Due to the cooperativity, many supramolecular architectures are far more stable than what would be expected from the consideration of individual binding sites alone.[28] The theoretical elucidation of the physical forces governing noncovalent interactions and their cooperativity thus is essential for the understanding of the base-pair stacking in DNA, inhibitions of drugs in enzymes, protein folding, molecular self-assembly, and crystal packing in nanoparticles and organic solids. This accumulated understanding and knowledge can also be used to guide the rational design of self-assembling molecules and the development of force fields which ultimately are applied to *in silico* simulations of the molecular assembling processes.[29]

Obviously, the most important and ubiquitous noncovalent and directional interaction in chemistry and biology is hydrogen bonding, which is the driving force for the DNA double helix structures and many self-assembling materials.[30−35] Its directionality particularly interests and encourages chemists to precisely control and rationally design complementary hosts for any given guest. The strength of hydrogen bonds ranges from a few kcal/mol, which is of the magnitude of van der Waals interactions and is mainly electrostatic in nature, to dozens of kcal/mol, which is comparable to the energy of a formal chemical bond and thus of major covalent contribution,[36−40] leading to the claim that hydrogen bonding is an interaction without borders.[41] In general, charged hydrogen bonds are much stronger than the hydrogen bonding

Received: August 31, 2019
Published: October 21, 2019

DOI: 10.1021/acs.joc.9b02381
J. Org. Chem. 2019, 84, 14805−14815

among neutral molecules. Significantly, multiple hydrogen bonds are in fact responsible for many recognition processes in nucleic acids, and dimers with multiple hydrogen bonds have been increasingly used in the design of supramolecular polymers[42,43] and DNA and RNA base pairs.[42,44,45]

In 1967, Rich and co-workers studied the binding in triply hydrogen-bonded dimers and found the stabilities for these dimers to be very different.[46] To explain the very different binding strengths in different complexes with the same number and types of hydrogen bonds, Jorgensen and Pranata computationally analyzed the cytosine-guanine (C-G) and uracil-2,6-diaminopyridine (U-DAP) complexes and proposed that it is inadequate to consider only primary electrostatic interactions and there is a need to introduce the concept of secondary electrostatic interaction (SEI).[47,48] As shown in Figure 1a, if the hydrogen bonding donors and acceptors are

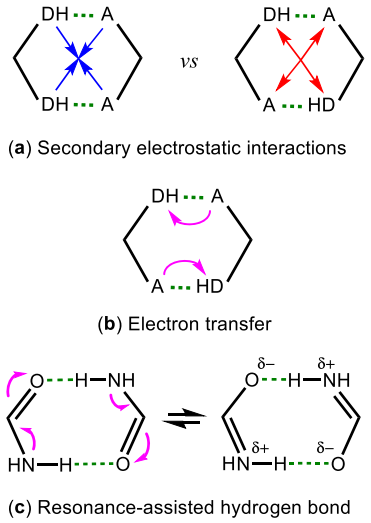

Figure 1. (a) Illustration of secondary electrostatic interactions (attraction in blue and repulsion in red). (b) Cooperativity of the electron transfer interactions. (c) Resonance-assisted hydrogen bond (RAHB).

aligned in the same respective sides, there is additional diagonal electrostatic attraction among adjacent hydrogen bonds (in blue), leading to the enhanced stability. However, if they are aligned alternatively, there is diagonal electrostatic repulsion among hydrogen bonds (in red), causing the instability. Following the SEI model, a DDD-AAA complex would have the highest association constant. This triply hydrogen-bonded system was later experimentally verified,[49−51] and various quadruple complexes of DDAD-AADA,[52] $(DDAA)_2$ and $(DADA)_2$,[53] and DDDD-AAAA[54] were also analyzed and compared. Based on the SEI model, the strength of the multiple hydrogen bonds would follow the order, DDDD-AAAA (DDD-AAA) > DDAA-AADD (DDA-ADD) > DADA-ADAD (DAD-ADA), because the SEIs are all attractive when all donors (or acceptors) are grouped together on one monomer. Since then, the SEI model has been validated by a plethora of experimental studies;[28,50,51,54−57] the DDDD-AAAA quadruple hydrogen bond array was reported to exhibit exceptionally large association constant. The SEI model has also been introduced in organic chemistry and supramolecular chemistry textbooks[58,59] to explain and predict the relative strength of similar self-assembly complexes.[58,59]

While experimental binding strengths are mostly in line with the simple SEI model,[47,48] further studies indicate that the SEI model is oversimplified, as the predictions are not always in line with the experimental data and there have been cautions for the use of the SEI model.[60−68] Other factors, such dipole−dipole attraction between monomers,[69,70] π resonance assistance,[39,40,71−74] σ induction or even long-range electrostatic interactions,[60,63] may all contribute to the cooperativity of multiple bindings. For instance, both experiments[75,76] and computations[77] have shown that amides (lactams) have stronger self-associations than imides, in accord with the SEI model. However, most recently Vallejo Narváez et al. questioned the role of the SEI and proposed that the balance between the acidity of the H-bond donor (N−H group) and the basicity of the HB acceptor (C═O group), which arises from the resonance effect of the spectator carbonyl, should be the primary cause for this phenomenon.[67] Similarly, van der Lubbe et al. found the correlation between the accumulation of charge around the frontier atoms and the binding energies,[68] but we note that the cause for the changes of the frontier atoms (either in acidity/basicity or charge density) need to be clarified. Our analyses, in the meanwhile, indicate that there are three major forces, namely, the σ induction effect (IE), π resonance effect (RE), and secondary electrostatic interaction (SEI), contributing to the different binding energies in the dimers of amides and imides.[65] It is interesting to note that Wu et al. found the correlation between the associations of multipoint hydrogen-bonded arrays and the aromaticity of cyclic rings in arrays upon complexation.[61] It is unclear, however, whether the aromaticity (electron delocalization) leads to the variations of the overall π resonance and the polarity (dipole moment) of monomers, and subsequently the dipole−dipole interaction among monomers. We also note that if electron transfer instead of electrostatics plays a significant or even decisive role in hydrogen bonding, there would be a cooperative rather than anticooperative effect for complexes of alternating multiple hydrogen bonds (Figure 1b),[78] and this is in conflict with the prediction by the SEI model.

Among various hydrogen bonds, the resonance-assisted hydrogen bond (RAHB, as shown in Figure 1c), which was first observed in the crystal structures of β-diketo enols by Gilli and co-workers,[39,40,71,74,79] may be the most attractive one as it highlights the interplay between resonance and hydrogen bonding. In RAHB systems, π electrons move from the H-bond donor to the acceptor through π conjugation, leading the donor to be more positive (i.e., reduction of the electron density or enhancement of the acidity) and the acceptor more negative (i.e., increase of the electron density or enhancement of basicity), and ultimately much stronger H-bonding than others without π conjugation. The RAHB concept was critically validated by us recently.[80,81] Furthermore, if the π conjugation goes in reverse from the H-bond acceptor to the donor, the H-bonding would be weakened by resonance, namely, resonance-inhibited (or impaired) hydrogen bond (RIHB).[82−84] Thus, it would be interesting and valuable to examine the role of π conjugation in multiple hydrogen bonding complexes where H-bonds are connected through π conjugation in monomers.

In this work, we aim to seek an improved understanding of the nature of the multiple hydrogen bonding complexes by quenching the π electron delocalization among hydrogen bond donors and acceptors. In this way, the energetic and structural

DOI: 10.1021/acs.joc.9b02381
J. Org. Chem. 2019, 84, 14805−14815

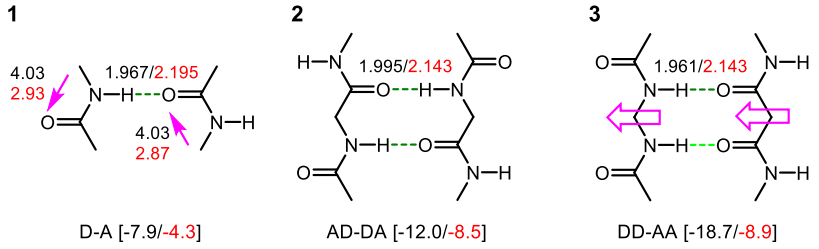

Figure 2. Interaction energies (in kcal/mol) and hydrogen bond distances (in Å) in the singly (**1**) and doubly (**2** and **3**) hydrogen-bonded complexes. The black values refer to regular DFT results, whereas the red ones are from the BLW method which strictly localizes π electron pairs on each donor and acceptor. Pink arrow with values refers to the dipole moments (in Debye).

changes can reflect the precise role of the π resonance effect. This is achieved by using the block-localized wave function (BLW) method,[85,86] which is the simplest and most efficient variant of valence bond (VB) theory[87−91] and can self-consistently derive the wave function for a strictly electron-localized (usually the most stable resonance) state. The BLW not only has the capability for geometry optimization with spectroscopic and magnetic properties computed, but also performs energy decomposition analysis where the hydrogen bonding energy can be decomposed to a number of energy components.

2. COMPUTATIONAL METHODS

2.1. Block-Localized Wave function (BLW) Method. Different from the philosophy of molecular orbital (MO) theory which uses delocalized MOs as building blocks for the molecular wave function, valence bond (VB) theory starts with localized atomic or fragmental orbitals to construct wave functions for Lewis (localized or resonance) structures, and the final molecular wave function is composed of several Lewis structures with the computational algorithm similar to the MCSCF within the MO theory.[87−91] Since a VB wave function is defined with a Heitler-London-Slater-Pauling (HLSP) function, which is composed of a series of Slater determinants, the computational complexity deters the development and broad applications of VB methods. To simplify the VB computations and combine the advantages of both MO and VB theories, we proposed the BLW method where a BLW is defined with a Slater determinant (a MO feature) and localized fragmental orbitals (a VB feature). In brief, it is assumed that for a molecular system, all electrons and primitive basis functions can be partitioned to k subgroups (blocks), and each orbital is block-localized and expanded in only one block. Orbitals in the same subspace are subject to the orthogonality constraint (a MO feature), but orbitals from different subspaces are nonorthogonal (a VB feature). The final BLW can be self-consistently optimized by minimizing its corresponding energy, and all localized orbitals are thus optimal. In general, a BLW is designated for the most stable resonance state in order to analyze the geometric, energetic, and spectral changes due to the electron delocalization in a molecule. The BLW method is available at the DFT level with the geometry optimization and frequency computation capabilities.[86]

In this work, the BLW state, in which the π electron pairs are strictly localized on each donor and acceptor, is defined as

$$\Psi_{HB}^{BLW} = \hat{A}\{\Phi\varphi_{D_1}^2 \cdots \varphi_{D_k}^2\varphi_{A_1}^2 \cdots \varphi_{A_k}^2\} \quad (1)$$

where $\{\varphi\}$ are block-localized MOs, and D and A refer to hydrogen bond donors and acceptors, respectively. Φ represents all remaining orbitals.

2.2. BLW Energy Decomposition (BLW-ED) Approach. Numerous energy decomposition analysis (EDA) approaches such as the Morokuma scheme,[92,93] EDA-NOCV,[94,95] and SAPT[96] have been proposed and widely applied in the exploration of chemical bonding nature.[97] Here, we used the EDA approach based on the BLW method (BLW-ED) which analyzes the intermolecular interactions by treating every monomer as a block.[98] In the BLW-ED approach, the interaction energy (ΔE_{int}) in a complex is decomposed into several chemically meaningful energy components, including steric (ΔE_s), polarization (ΔE_{pol}), charge transfer (ΔE_{CT}), and dispersion correction (ΔE_{disp}) as

$$\Delta E_{int} = \Delta E_s + \Delta E_{pol} + \Delta E_{CT} + \Delta E_{disp} \quad (2)$$

Noted that here the steric term involves electrostatic and Pauli repulsive interactions and even electron correlations at the DFT level, whereas the correction of basis set superposition errors (BSSE) with the counterpoise method proposed by Boys and Bernardi[99] is included in the charger transfer energy component. Besides, the dispersion correction represents the difference of Grimme's correction (D3)[100,101] between the dimer and the sum of each monomer.

$$\Delta E_{disp} = E_{disp}^{Dimer} - E_{disp}^{A} - E_{disp}^{B} \quad (3)$$

2.3. Computational Details. Since the Minnesota M06-2X exchange-correlation functional[102] can correctly reproduce non-covalent interactions in organic molecules,[103−105] DFT(M06-2X-D3) computations with the basis set of 6-311+G(d,p) were performed throughout the work with the in-house version of GAMESS software[106] to which our BLW code is ported. The comparison of the geometrical parameters and interaction energies computed with the standard DFT and the BLW method (at the same DFT level) reveals the impacts of the π resonance on multiple hydrogen bonding. All interaction energies including DFT and BLW methods were improved with the BSSE and Grimme's dispersion corrections.

3. RESULTS AND DISCUSSION

3.1. Single and Double Hydrogen Bonding. We first examined the hydrogen bond between two methylacetamide molecules (**1**) which can be used as a reference for the doubly hydrogen-bonded complexes **2** and **3**, as shown in Figure 2. We note that the general validation of the SEI concept was presented by these two dipeptide models in Jorgensen's original paper,[47] as the resonance between the two peptide bonds in each monomer is disabled by the in-between methylene group. For the individual peptide bond, however, there is considerable π conjugation from the amine group to the carbonyl group leading to the planarization of the amine group. This π resonance nearly doubles the hydrogen bonding strength in **1** from 4.3 to 7.9 kcal/mol. It would be expected that the hydrogen bonding in dipeptide models be two times the strength in **1**, or around 15.8 kcal/mol. DFT computations show that the bonding energies in **2** and **3** are 12.0 and 18.7 kcal/mol, respectively. Energy decomposition analyses (see Table 1) further confirm that the charge transfer energy is essentially the same in both dipeptide complexes, indicating the minor cooperativity in charge transfer interactions as shown in Figure 1b. The energy difference between **2** and **3** comes from the steric and polarization interactions, both of

DOI: 10.1021/acs.joc.9b02381
J. Org. Chem. 2019, 84, 14805−14815

Table 1. Energy Components to the Total Interaction Energy (in kcal/mol) at the M06-2X-D3/6-311+G(d,p) Level with the BLW-ED Method

complex	ΔE_{int}	ΔE_s	ΔE_{pol}	ΔE_{CT}	ΔE_{disp}
1	−7.9	−4.6	−1.9	−1.0	−0.4
2	−12.0	−6.2	−2.8	−2.1	−0.9
3	−18.7	−10.9	−4.8	−2.1	−0.9
4	−30.9	−12.1	−10.8	−7.5	−0.5
4′	−26.6	−10.5	−9.1	−6.7	−0.3
5	−18.3	−5.7	−5.6	−6.5	−0.5
5′	−18.2	−4.4	−6.1	−7.4	−0.3
6′	−14.0	−8.6	−2.9	−2.1	−0.4
7	−46.0	−21.5	−15.9	−7.8	−0.8
7′	−40.4	−22.8	−11.4	−5.7	−0.5
8	−15.6	−7.9	−4.1	−2.8	−0.8
8′	−23.4	−11.7	−6.8	−4.0	−0.9
9	−68.8	−14.6	−32.5	−20.8	−0.9
9′	−36.8	−13.8	−13.4	−9.0	−0.6
10	−27.9	−8.8	−9.0	−9.2	−0.9
10′	−20.6	−5.9	−6.0	−8.2	−0.6
11′	−21.9	−13.4	−4.8	−3.0	−0.7
12	−59.2	−26.4	−21.1	−10.1	−1.6
12′	−30.7	−14.3	−9.4	−5.5	−1.5
13	−46.9	−27.0	−12.1	−7.1	−0.7

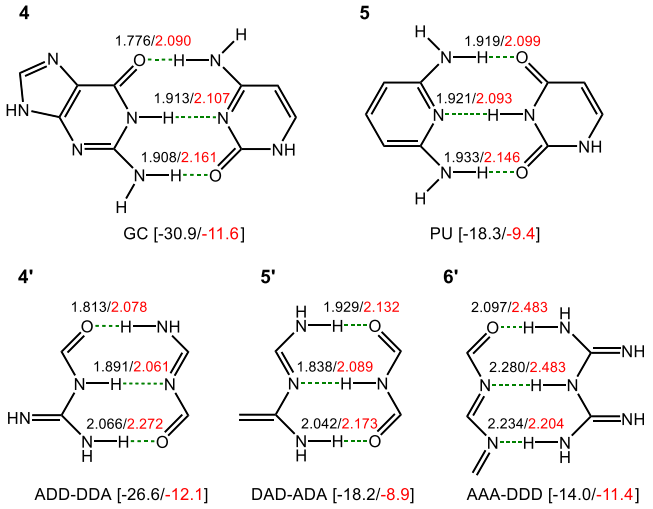

Figure 3. Interaction energies (in kcal/mol) and hydrogen bond distances (in Å) in the GC and PU pairs and their linear analogues. The black values refer to regular DFT results, whereas the red ones are from the BLW method which strictly localizes π electron pairs on each donor and acceptor.

which favor **3**. But can this difference (6.7 kcal/mol) be fully assigned to the SEI effect?

To justify the precise role of π resonance in the bonding in these dipeptide models, we applied the BLW method to reoptimize the geometries of AD-DA (**2**) and DD-AA (**3**), where the each π electron pair is strictly localized either on the carbonyl group or on the amine group. The deactivation of π resonance results in the elongation of the H-bonding distances for both **2** (from 1.995 to 2.143 Å) and **3** (from 1.961 to 2.143 Å), confirming the RAHB concept. Note that the H-bonding distances in **2** and **3** are essentially the same in BLW optimizations, and the bonding strengths are 8.5 and 8.9 kcal/mol, respectively. Both energy values are close to 8.6 kcal/mol, which is two times the single hydrogen bonding energy in **1** without π resonance. The small energy difference (0.4 kcal/mol) can be assigned to the SEI effect completely. Thus, the RAHB is the driving force for the binding energy difference in doubly hydrogen-bonded complexes and the SEI plays a secondary role. One consequence of the conjugation is the variations of molecular polarities (dipole moments). The π conjugation from the amine group to the carbonyl group increases the dipole moment in methylacetamide as shown in Figure 2. In dipeptides, along the hydrogen bonding direction the local dipoles can either reinforce (as in **3**, see the arrows in pink) or cancel out (**2**), depending on their orientations in each peptide bonds. Obviously, RAHB increases the dipole moments which favor the electrostatic attraction in **3**.

3.2. Triple Hydrogen Bonding. We continued to examine the DNA pairs guanine-cytosine (GC, **4**) and 2,6-diaminopyridine-uracil (PU, **5**) which have been well studied in the literature and are shown in Figure 3. Computational results show that the GC pair with the ADD-DAA motif has an interaction energy of −30.9 kcal/mol, while the interaction energy for the PU pair with the DAD-ADA motif is only −18.3 kcal/mol. The GC pair thus is more stable than the PU pair by 12.6 kcal/mol, which is consistent with the experimental observation. As we can see, the GC pair has one repulsive plus one attractive SEI, while PU pair owns two repulsive SEIs. Accordingly, the energetic difference can be well rationalized by the SEI model. However, in all four nucleobases there are aromatic rings involved. Thus, there is a proposal that the binding energy difference between the GC and PU pairs may be due to the difference in the aromaticity, as the GC pair has more "aromaticity gain" than the PU pair.[61] To single out the role of aromaticity in DNA binding, we removed the aromatic rings and considered their linear analogues **4′** and **5′** with results shown in Figure 3. Still, the ADD-DAA array **4′** is 8.4 kcal/mol more stable than DAD-ADA array **5′**, suggesting that the energetic difference would occurs even without the "aromaticity gain".

To further clarify the driving forces for the differences in hydrogen bonding strengths and distances, the BLW method was applied to reoptimize all dimers shown in Figure 3. In the BLW state, the π electron pairs on each donor and acceptor are strictly localized; thus, the π conjugation is completely "shut down". While the interaction energies are dramatically reduced (red data in Figure 3), confirming the concept of RAHB, the difference between the GC and PU pairs surprisingly decreases to only 2.2 kcal/mol (compared to 12.6 kcal/mol with the π resonance on). More significantly, the BLW interaction energies for the electron-localized states of **4** (−11.6 kcal/mol) and **5** (−9.4 kcal/mol) are very close to those in **4′** (−12.1 kcal/mol) and **5′** (−8.9 kcal/mol), respectively. Thus, the large differences in the interaction energies between the GC and PU pairs are dominated by the π resonance. Based on the hydrogen bonding distances derived from the BLW method (2.090/2.107/2.161 Å for **4** and 2.099/2.093/2.146 Å for **5**), the interaction energy in **5** would be expected to be close to or even higher than that in **4**, but there is the SEI which is more repulsive in **5**, leading to the lower interaction energy in **5** than in **4** by 2.2 kcal/mol. This small energy gap suggests that the SEI plays only a minor role in the DNA pairs. In other words, *the multiple hydrogen bonding can be viewed as a kind of resonance-assisted hydrogen bond (RAHB), in which π resonance occurs in monomers.* There are two impacts from the π conjugation in the present cases. One is the charge

DOI: 10.1021/acs.joc.9b02381
J. Org. Chem. 2019, 84, 14805−14815

accumulations (or the changes of acidity/basicity) on the hydrogen bond acceptors (more negative) and donors (more positive) as illustrated in Figure 1c, resulting in the enhancement of hydrogen bonds. The other is the change of the polarity (dipole moment) of a monomer due to the π electron movement. In the GC pair, the conjugation results in the increasing of the polarity of monomers (from 4.22 to 7.25 D for G and from 4.24 to 6.14 D for C) perpendicular to the hydrogen bonding direction, and the polarities in G and C are opposite to each other, leading to the favorable electrostatic attraction. Differently, there is no change of polarity perpendicular to the bonding direction for P and U in the PU pair. Thus, there is no additional electrostatic attraction between P and U due to the π conjugation.

If resonance is responsible for the enhancement of the triple hydrogen bonding, the AAA-DDD array, which is predicted to have the maximum interaction energy based on the SEI hypothesis, would be the most unstable one. This is because the π resonance effect is insignificant in the AAA-DDD array since all donors are grouped into one monomer whereas all acceptors are grouped into the other monomer. To validate our view, the model molecule **6′** with the AAA-DDD motif, shown in Figure 3, was studied. As expected, the energetic difference between the regular DFT and BLW method is only 2.6 kcal/mol. Therefore, the lowest interaction energy for **6′** (−14.0 kcal/mol, compared with −26.6 kcal/mol in **4′** and −18.2 kcal/mol in **5′**) strongly disfavors the popular SEI hypothesis but endorses our resonance explanation. With the π conjugation "turned off", however, the interaction energies for linear **4′** (−12.1 kcal/mol), **5′** (−8.9 kcal/mol), and **6′** (−11.4 kcal/mol) are quite close, and the deviations particularly for **5′** most likely result from the polarities of monomers.

The π conjugation can be better depicted with the electron density difference (EDD) maps, which exhibit the difference between an electron-delocalized (DFT) and its corresponding electron-localized (BLW) states in total densities. Figure 4

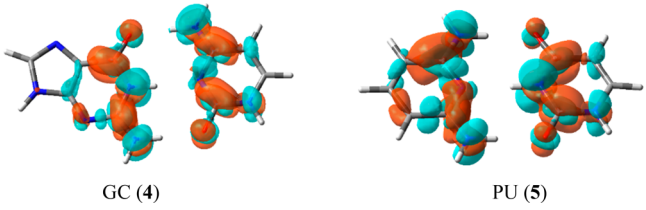

Figure 4. Electron density difference (EDD) isosurface maps with the isovalue of 0.004 au showing the movement of electron density due to π conjugation in **4** and **5**. The orange/cyan colors indicate increasing/decreasing of the electron density.

plots the EDD maps for **4** and **5**. As expected, there is π electron density gain in acceptors and loss in donors due to the π resonance. This clearly confirms the nature of resonance assistance in the multiple hydrogen bonding.

To visualize and compare the change of the electrostatic energy in triple hydrogen-bonded arrays with the π resonance "turned on" and "turned off", we plotted out the electrostatic potential surfaces (EPSs) of the GC and PU pairs in Figure 5. It is very obvious that from the electron-localized BLW state to the electron-delocalized DFT state for a molecule with the resonance assistance, the boundary between the H-bond donor and acceptor gets greener or even bluer, suggesting the enhancement of the electrostatic attraction between the two

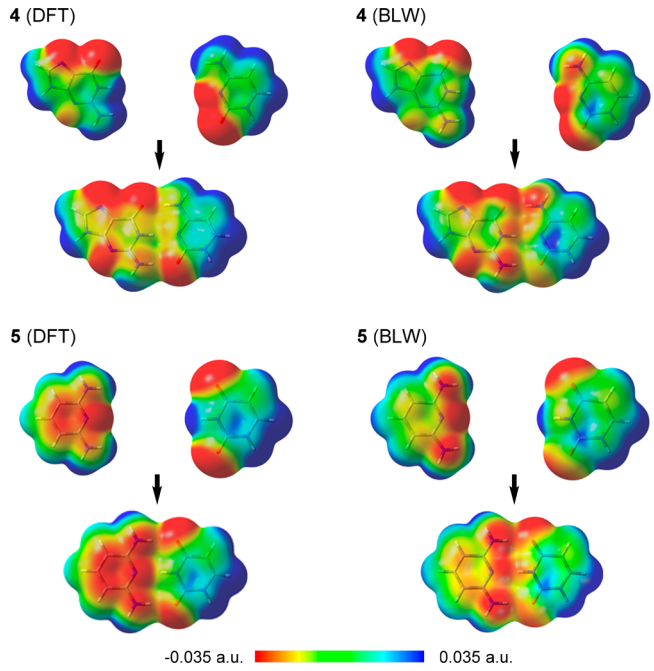

Figure 5. Electrostatic potentials on the 0.001 au electron density surfaces of complexes **4** (GC pair) and **5** (PU pair) computed at the M06-2X/6-311+G(d,p) level.

groups. In addition, the EPSs for **4** and **5** in BLW states exhibit very similar electrostatic distribution on frontier atoms of donors and acceptors, which also rationalizes that the charge accumulation difference[68] between monomers in **4** and **5** mainly comes from the resonance effect.

However, Blight et al. reported that both neutral and cationic DDD-AAA arrays have exceptional strong binding strength.[51,54] To address the discrepancy between our theoretical analyses above and experimental findings, we studied the model complex **7** as shown in Figure 6. Consistent with the experimental observation, the interaction energy for **7** (−46.0 kcal/mol) is indeed much higher than those for **4** and **5** (Figure 3). Yet, the hydrogen bonding distances in **7** are very close to the values in **5** and even longer than those in **4**, which should result in a relatively lower interaction energy. A similar situation was also observed in its linear analogue **7′** (see Figure 6) of the DDD^+-AAA array, for which the interaction energy is −40.4 kcal/mol but with reduced hydrogen bonding distances compared with **4′** and **5′**. Obviously, the differences can be ascribed to the positive charge. In fact, among the recently identified strong and unconventional hydrogen bonds is the charge assisted hydrogen bond (CAHB) where the donor group has a positive charge or the acceptor group has a negative charge.[73,107,108] Since the hydrogen bond is primarily dominated by electrostatic interaction, the positive charge in DDD^+ monomer would enhance the electrostatic attraction significantly. Subsequent BLW-ED analyses confirmed our claim, as the contributions from the electrostatic interaction are much larger for **7** and **7′** than for other systems (see following Table 1). Nevertheless, for the neutral DDD-AAA array **8** (shown in Figure 6) where the positive charge in **7** is replaced with a hydrogen atom, the interaction energy remarkably decreased to −15.6 kcal/mol, which is very close to the linear DDD-AAA array **6** (−14.0 kcal/mol). With the resonance "shut down", both the hydrogen bond distances and interaction energies in **7** and **7′** experience little change. This

DOI: 10.1021/acs.joc.9b02381
J. Org. Chem. 2019, 84, 14805−14815

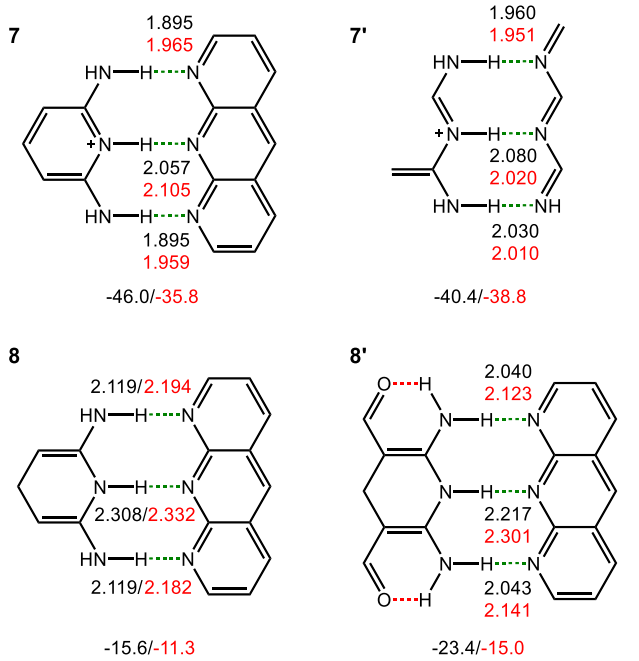

Figure 6. Interaction energies (in kcal/mol) and hydrogen bond distances (in Å) for **7** and **8**. The black values refer to regular DFT results, whereas the red ones are from the BLW method which strictly localizes π electron pairs on each donor and acceptor.

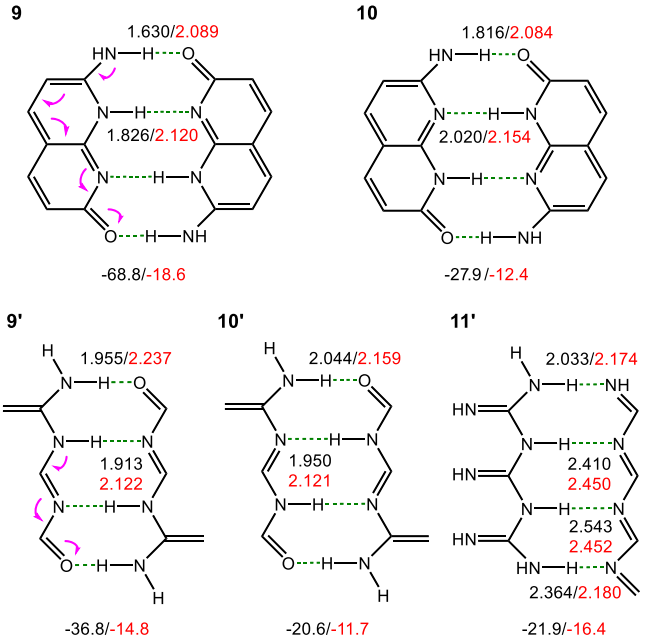

Figure 7. Interaction energies (in kcal/mol) and hydrogen bond distances (in Å) for quadruple hydrogen-bonded arrays **9**−**11**. The black values refer to regular DFT results, whereas the blue ones are from the BLW method which strictly localizes π electron pairs on each donor and acceptor.

further proves that the much stronger hydrogen bonding in cationic DDD-AAA complexes simply results from the positive charge. Of course, adding electron-withdrawing groups to hydrogen bond donors can modulate the hydrogen bonding as well. By introducing two carbonyl groups to **8**, we can design complex **8′** shown in Figure 6 whose interaction energy increases to −23.4 kcal/mol. This is because the π electrons conjugated from hydrogen bond donors ($-NH_2$) to the substituent carbonyl groups lead the donors to being more positively charged and ultimately enhance the hydrogen bonding. Thus, the hydrogen bonds in DDD-AAA arrays can be tuned by either introducing positive charges or adding electron-withdrawing groups through the π conjugation to the hydrogen bond donors.

3.3. Quadruply Hydrogen Bonding. The resonance explanation can also be used to rationalize the nature of the quadruple hydrogen bond and the relative stability of dimers with different arrays (Figure 7). Tautomeric complexes **9** and **10** have the same number of hydrogen bonds but very different interaction energies and hydrogen bond distances. The interaction energy in **9** is more than 40 kcal/mol higher than in **10**. If we remove the aromatic rings and construct their linear analogues **9′** and **10′**, the interaction energies would be reduced from −68.8 to −36.8 kcal/mol and from −27.9 to 20.6 kcal/mol, respectively. In other words, the interaction energy difference would also be reduced from more than 40 to about 16 kcal/mol. To investigate the cause for the energy differences in both aromatic (**9** and **10**) and linear (**9′** and **10′**) complexes, we again applied the BLW method. With the π resonance "shut down", the interaction energies for **9** and **10** become −18.6 kcal/mol and −12.4 kcal/mol, respectively, again confirming the dominant role of the π resonance effect. Besides, the hydrogen bond distances are nearly unchanged for **9** and **10** in BLW geometries. With π electrons strictly localized, **9′** is only 3.1 kcal/mol more stable than **10′**, though the hydrogen bond distances in **10′** (2.159 and 2.121 Å) are a little shorter than those in **9′** (2.237 and 2.122 Å). This discrepancy between the interaction energies and bonding distances can be ascribed to the SEI, which is more repulsive in **10′**. It should be noted that there is a coupling effect between resonance and SEI, as the latter can be enhanced by the π resonance from hydrogen bond donor to acceptor which leads to extra positive charge on the donor side and extra negative charge on the acceptor side. As for **11′** with the DDDD-AAAA array, in contrast to the prediction by the SEI hypothesis, it is not the most stable one among **9′**−**11′**. The interaction energy for **11′** is much lower than that for **9′** but nearly identical to **10′** when the π resonance is on with DFT results, but it is indeed higher than both **9′** and **10′** when the π resonance is off with BLW results. Thus, our computations confirm the order of the multiple hydrogen bonding strengths as DDDD-AAAA (**11′**) > DDAA-AADD (**9′**) > DADA-ADAD (**10′**), only when the π resonance is "turned off". Again, the π resonance effect is the primary factor governing the relative strengths in various multiple hydrogen-bonded arrays with partial contribution from SEI.

If we compare the neutral quadruple hydrogen bonding complexes (Figure 7) with the triple hydrogen bonding complexes (Figure 3), all the interaction energies are approximately proportional to the number of hydrogen bonds, except the energy in **9** which is exceptionally high (−68.8 kcal/mol), in line with the "aromaticity gain" claim.[61] However, if we look at the π conjugation pathway, **9** is the only one where the π electrons can move from the top electron donating amine group to the down electron withdrawing carbonyl group as highlighted with purple arrows in Figure 7. The much longer π electron migration in **9** than in **10** can be examined by both dipole moments and the EDD maps as shown in Figure 8. From the EDD maps, we can see that the π resonance goes from the donors to the acceptors for both **9**

DOI: 10.1021/acs.joc.9b02381
J. Org. Chem. 2019, 84, 14805−14815

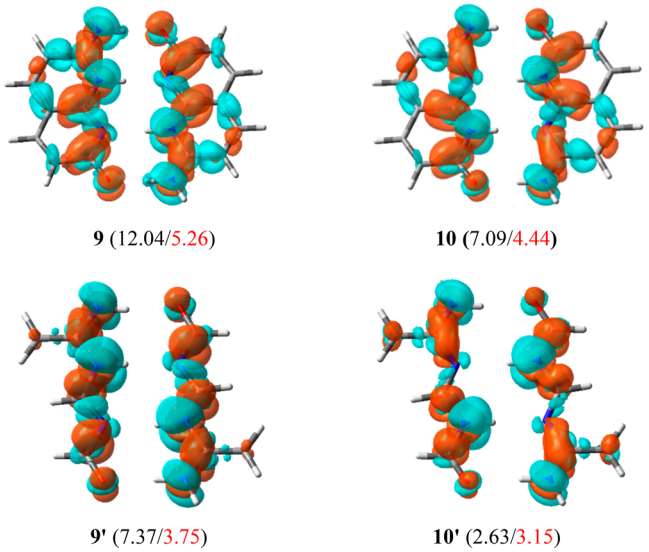

Figure 8. Molecular dipole moments (in bracket, Debye. Black/red values refer to DFT/BLW results) for monomers and electron density difference (EDD) isosurface maps with the isovalue of 0.004 au showing the movement of electron density due to π conjugation in **9**, **10**, **9′**, and **10′**. The orange/cyan colors indicate increasing/decreasing of the electron density.

and **10**, resulting in the hydrogen bond donors being more positive and acceptors more negative, and subsequently much stronger hydrogen bonding. It is obvious that there is a larger charge accumulation around the frontier atoms in the DDAA motif (**9**) than that in the DADA motif (**10**), due to the resonance effect. Therefore, the hydrogen bonding in the former is much stronger than in the latter, as discussed in the literature.[68] Figure 9 shows the electrostatic potential surfaces

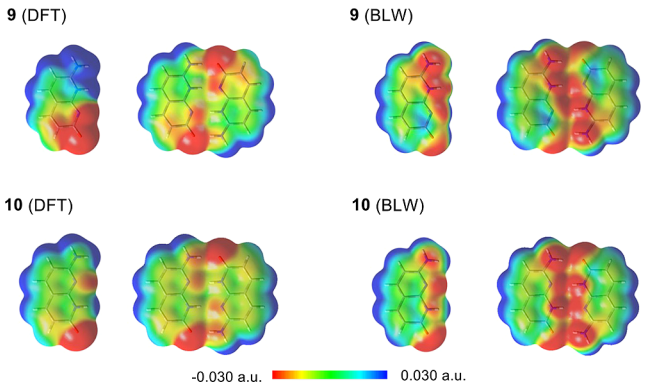

Figure 9. Electrostatic potentials on the 0.001 au electron density surfaces of complexes **9** and **10** computed at the M06-2X/6-311+G(d,p) level.

(EPSs) for **9** and **10**. The significant change from monomer to complex in **9** (DFT) indicates the strong electrostatic attraction and polarization stability in the hydrogen bonding, apart from the electron transfer.

At last, we analyzed the dimer with all hydrogen bond donors on one monomer and all acceptors on the other monomer, i.e., DDDD-AAAA, as shown in Figure 10. Both the aromatic (**12**) and linear (**13**) dimers with one positive charge on the DDDD motif exhibit exceptional large interaction energies, which is consistent with the literature.[54] However, the hydrogen bond distances for the DDDD$^+$-AAAA array are longer than those for its corresponding DDAA-AADD and DADA-ADAD arrays. This can also be explained by the enhanced electrostatic interaction due to the positive charge. Unsurprisingly, by removing the positive charge, interaction energies dramatically decrease from −59.2 kcal/mol to −30.7 kcal/mol for aromatic dimers and from −46.9 kcal/mol to −21.9 kcal/mol (**11′** in Figure 7) in linear dimers.

3.4. Energy Decomposition Analysis. As a last step, we performed the BLW-ED calculations to further understand the driving forces in the above multiple hydrogen bonding complexes **1**−**13** from the perspectives of monomers with results compiled in Table 1. All three components including the steric energy, polarization energy, and charge transfer energy make notable contributions to the binding complexes. Considering that the steric energy is composed of the Pauli repulsion and the electrostatic interaction and plays a stabilizing role in all complexes, we can derive that the electrostatic interaction is very attractive. Notably, for **5** (**5′**) and **10** (**10′**) with DAD and DADA motifs, the contribution of the charge transfer (σ-CT) is the largest, implying the significant covalent nature in hydrogen bonding. The most important finding is that the complexes with DD(DD)-AA(AA) arrays (including **3**, **6**−**8**, and **11**−**13**) have the largest contribution from the steric effect, i.e., electrostatic attraction, in line with the SEI model.

In the pretext, we ascribed the large binding energy differences between **2** and **3** and between **4** and **5** to π resonance. Indeed, the charge transfer stability through σ-channels in these two pairs (and the linear analogous **4′** and **5′**) is very close, in agreement with their similar hydrogen bonding distances. The enhanced electrostatic attraction and polarization in **3** or **4** or **4′**, which result from the π conjugation within monomers, are responsible for the much higher interaction energy compared with **2** or **5** or **5′**, respectively. Owing to the assistance from the π conjugation, the steric energy (or electrostatic attraction) in **4′** is even higher than in **6′**, which is of the DDD-AAA array and whose charge transfer stabilization is the lowest due to the elongated hydrogen bonding distances. As expected, electrostatic attraction dominates the charged hydrogen bonds in both **7** and **7′**. Due to the lack of effective π conjugation in **8**, not only the total interaction energy but also the energy components in **8** are very similar to the case of **6′**. Adding electron-withdrawing groups to **8** would notably increase the electrostatic attraction associated with the polarization in **8′**. The extremely high charge transfer and polarization stabilization energies in **9** are very notable. The high charge transfer energy can be traced to its short hydrogen bonding distances as shown in Figure 7, while the high polarization energy in **9** indicates its strong and long π resonance pathway. It is interesting to note that the steric effect is essentially the same in **9** and its linear analogue **9′** and does not contribute to their huge interaction energy difference. Like **7** and **7′**, **12** and **13** are overwhelmed by the electrostatic attractions due to the positive charge in the side of hydrogen bond donors.

4. CONCLUSIONS

Multiple hydrogen bonding arrays play a fundamental role in supramolecular chemistry. In order to explain and predict the relative hydrogen bonding strength in self-assembled complexes, the secondary electrostatic interaction (SEI) model was proposed and has been widely utilized. Recent extensive

DOI: 10.1021/acs.joc.9b02381
J. Org. Chem. 2019, 84, 14805−14815

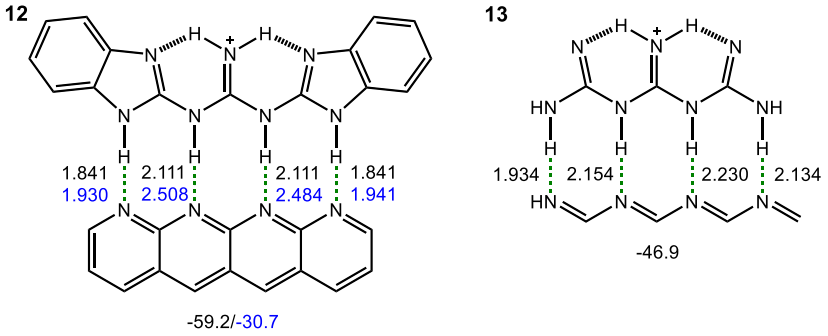

Figure 10. Interaction energies (in kcal/mol) and hydrogen bond distances (in Å) for **12** and **13**. The black values refer to the cationic array, whereas blue values represent the neutral analogy by removing the positive charge and one hydrogen atom.

studies, however, have questioned the validity of this simple model. In this work, we used the simplest variant of VB theory, the block-localized wave function (BLW) method, to study the interaction in a series of exemplary doubly, triply, and quadruply hydrogen-bonded complexes where hydrogen bond donors and acceptors are connected via π conjugation. The significance of the BLW method lies in its capability to derive strictly electron-localized states where the π conjugation is "shut down". By comparing the geometries and energetics of both electron-delocalized and electron-localized states for the very same complex, we can differentiate and clarify the roles of SEI and π conjugation in multiple hydrogen bonding.

Our BLW computations show that the fundamental driving force is the resonance-assisted hydrogen bond (RAHB), and the hydrogen bonding strengths can be significantly enhanced by the π conjugation from the hydrogen bond donors to acceptors, which leads to the donors having more positive charges and the acceptors being more negatively charged. By quenching the π resonance, the interaction energies would be significantly reduced for all studied systems except for the complexes with all donors grouped in one monomer and all acceptors grouped on the other monomer (i.e., D_n–A_n) where the π conjugation has a very limited impact. Therefore, in contrast to the prediction by the SEI model, D_n–A_n bonded arrays are not the most stable, as the resonance assistance is insignificant. With the π conjugation "shut down", however, the SEI model may work to a certain extent. This suggests that the SEI is secondary while the π resonance is the primary and decisive factor governing the multiply hydrogen-bonded complexes. The experimental findings that D_n–A_n bonded arrays exhibit exceptional large binding energies due to the fact that these arrays usually carry charges or electron-withdrawing substituent groups.

■ ASSOCIATED CONTENT

Supporting Information

The Supporting Information is available free of charge on the ACS Publications website at DOI: 10.1021/acs.joc.9b02381.

Comparison of BLW-ED results at the M06-2X-D3, B3LYP-D3, and HF levels for complexes **1**–**3**; electron density difference (EDD) isosurface maps and electrostatic potential maps for complexes **1**–**3**, together with all optimal geometries for complexes **1**–**13** (PDF)

■ AUTHOR INFORMATION

Corresponding Author

*E-mail: yirong.mo@wmich.edu

ORCID

Wei Wu: 0000-0002-6139-5443

Yirong Mo: 0000-0002-2994-7754

Notes

The authors declare no competing financial interest.

■ ACKNOWLEDGMENTS

This work was supported by the China Scholarship Council (for XL); the National Natural Science Foundation of China (No. 21733008 for W.W.) and Western Michigan University (for Y.M.).

■ REFERENCES

(1) Hobza, P.; Müller-Dethlefs, K. *Non-Covalent Interactions: Theory and Experiment*; Royal Society of Chemistry: London, 2009.
(2) Stone, A. J. *The Theory of Intermolecular Forces*; Oxford University Press: United Kingdom, 2013.
(3) Beno, B. R.; Yeung, K.-S.; Bartberger, M. D.; Pennington, L. D.; Meanwell, N. A. A Survey of the Role of Noncovalent Sulfur Interactions in Drug Design. *J. Med. Chem.* **2015**, *58*, 4383–4438.
(4) Zhao, F.; Ma, M. L.; Xu, B. Molecular Hydrogels of Therapeutic Agents. *Chem. Soc. Rev.* **2009**, *38*, 883–891.
(5) Webber, M. J.; Langer, R. Drug Delivery by Supramolecular Design. *Chem. Soc. Rev.* **2017**, *46*, 6600–6620.
(6) *Supramolecular Chemistry: From Molecules to Nanomateria*, 1st ed., Steed, J. W.; Gale, P. A., Eds.; Wiley-VCH: Weinheim, 2012.
(7) Fabbrizzi, L.; Poggi, A. Sensors and Switches from Supramolecular Chemistry. *Chem. Soc. Rev.* **1995**, *24*, 197–202.
(8) Sun, X.; James, T. D. Glucose Sensing in Supramolecular Chemistry. *Chem. Rev.* **2015**, *115*, 8001–8037.
(9) *Supramolecular Catalysis*, 1st ed., van Leeuwen, P. W. N. M., Ed.; Wiley-VCH: Weinheim, 2008.
(10) Vriezema, D. M.; Aragonès, M. C.; Elemans, J. A. A. W.; Cornelissen, J. J. L. M.; Rowan, A. E.; Nolte, R. J. M. Self-Assembled Nanoreactors. *Chem. Rev.* **2005**, *105*, 1445–1490.
(11) Daniel, M.-C.; Astruc, D. Gold Nanoparticles: Assembly, Supramolecular Chemistry, Quantum-Size-Related Properties, and Applications toward Biology, Catalysis, and Nanotechnology. *Chem. Rev.* **2004**, *104*, 293–346.
(12) *Supramolecular Soft Matter: Applications in Materials and Organic Electronics*, Nakanishi, T., Ed.; Wiley-VCH: Hoboken, NJ, 2011.
(13) Roy, N.; Bruchmann, B.; Lehn, J.-M. DYNAMERS: Dynamic Polymers As Self-Healing Materials. *Chem. Soc. Rev.* **2015**, *44*, 3786–3807.
(14) Yang, L.; Tan, X.; Wang, Z.; Zhang, X. Supramolecular Polymers: Historical Development, Preparation, Characterization, and Functions. *Chem. Rev.* **2015**, *115*, 7196–7239.
(15) Schneider, H.-J. Binding Mechanisms in Supramolecular Complexes. *Angew. Chem., Int. Ed.* **2009**, *48*, 3924–3977.

DOI: 10.1021/acs.joc.9b02381
J. Org. Chem. 2019, 84, 14805–14815

(16) Cavallo, G.; Metrangolo, P.; Milani, R.; Pilati, T.; Priimagi, A.; Resnati, G.; Terraneo, G. The Halogen Bond. *Chem. Rev.* **2016**, *116*, 2478−2601.
(17) Murray, J. S.; Lane, P.; Politzer, P. Simultaneous σ-Hole and Hydrogen Bonding by Sulfur- and Selenium-Containing Heterocycles. *Int. J. Quantum Chem.* **2008**, *108*, 2770−2781.
(18) Priimagi, A.; Cavallo, G.; Metrangolo, P. The Halogen Bond in the Design of Functional Supramolecular Materials: Recent Advances. *Acc. Chem. Res.* **2013**, *46*, 2686−2695.
(19) Pascoe, D. J.; Ling, K. B.; Cockroft, S. L. The Origin of Chalcogen-Bonding Interactions. *J. Am. Chem. Soc.* **2017**, *139*, 15160−15167.
(20) Gleiter, R.; Werz, D. B.; Rausch, B. J. A World Beyond Hydrogen Bonds? Chalcogen-Chalcogen Interactions Yielding Tubular Structures. *Chem. - Eur. J.* **2003**, *9*, 2676−2683.
(21) Zahn, S.; Frank, R.; Hey-Hawkins, E.; Kirchner, B. Pnicogen Bonds: A New Molecular Linker? *Chem. - Eur. J.* **2011**, *17*, 6034−6038.
(22) Bauzá, A.; Mooibroek, T. J.; Frontera, A. Tetrel-Bonding Interaction: Rediscovered Supramolecular Force? *Angew. Chem., Int. Ed.* **2013**, *52*, 12317−12321.
(23) Dougherty, D. A. Cation-π Interactions in Chemistry and Biology: A New View of Benzene, Phe, Tyr, and Trp. *Science* **1996**, *271*, 163−168.
(24) Schottel, B. L.; Chifotides, H. T.; Dunbar, K. R. Anion-π Interactions. *Chem. Soc. Rev.* **2008**, *37*, 68−83.
(25) Hunter, C. A.; Sanders, J. K. M. The Nature of π-π Interactions. *J. Am. Chem. Soc.* **1990**, *112*, 5525−5534.
(26) Sinnokrot, M. O.; Sherrill, C. D. High-Accuracy Quantum Mechanical Studies of π−π Interactions in Benzene Dimers. *J. Phys. Chem. A* **2006**, *110*, 10656−10668.
(27) Ercolani, G. Assessment of Cooperativity in Self-Assembly. *J. Am. Chem. Soc.* **2003**, *125*, 16097−16103.
(28) Prins, L. J.; Reinhoudt, D. N.; Timmerman, P. Noncovalent Synthesis Using Hydrogen Bonding. *Angew. Chem., Int. Ed.* **2001**, *40*, 2382−2426.
(29) Lopes, P. E. M.; Guvench, O.; MacKerell, A. D., Jr. In *Molecular Modeling of Proteins*, Kukol, A., Ed.; Springer: New York, 2015; Vol. *1215*, pp 47−71.
(30) Scheiner, S. Ab Initio Studies of Hydrogen Bonds: The Water Dimer Paradigm. *Annu. Rev. Phys. Chem.* **1994**, *45*, 23−56.
(31) Scheiner, S. *Hydrogen Bonding: A Theoretical Perspective*; Oxford University Press: New York, 1997.
(32) Jeffrey, G. A. *An Introduction to Hydrogen Bonding*; Oxford University Press: New York, 1997.
(33) Desiraju, G. R.; Steiner, T. *The Weak Hydrogen Bond In Structural Chemistry and Biology*; Oxford University Press: New York, 2001.
(34) Gilli, G.; Gilli, P. *The Nature of the Hydrogen Bond*; Oxford University Press: USA, 2009.
(35) Steiner, T. The Hydrogen Bond in the Solid State. *Angew. Chem., Int. Ed.* **2002**, *41*, 48−76.
(36) Cleland, W. W.; Kreevoy, M. M. Low-Barrier Hydrogen Bonds and Enzymic Catalysis. *Science* **1994**, *264*, 1887−1890.
(37) Frey, P. A.; Whitt, S. A.; Tobin, J. B. A Low-Barrier Hydrogen Bond in the Catalytic Triad of Serine Proteases. *Science* **1994**, *264*, 1927−1930.
(38) Lough, A. J.; Park, S.; Ramachandran, R.; Morris, R. H. Switching On and Off a New Intramolecular Hydrogen-Hydrogen Interaction and the Heterolytic Splitting of Dihydrogen. Crystal and Molecular Structure of $[Ir\{H(h1\text{-}SC_5H_4NH)\}_2(PCy_3)_2]BF_4\cdot 2.7CH_2Cl_2$. *J. Am. Chem. Soc.* **1994**, *116*, 8356−8357.
(39) Gilli, G.; Bellucci, F.; Ferretti, V.; Bertolasi, V. Evidence for Resonance-Assisted Hydrogen Bonding from Crystal-Structure Correlations on the Enol Form of the b-Diketone Fragment. *J. Am. Chem. Soc.* **1989**, *111*, 1023−1028.
(40) Bertolasi, V.; Gilli, P.; Ferretti, V.; Gilli, G. Evidence for Resonance-Assisted Hydrogen Bonding. 2. Intercorrelation between Crystal Structure and Spectroscopic Parameters in Eight Intramolecularly hydrogen-bonded 1,3-Diaryl-1,3-Propanedione Enols. *J. Am. Chem. Soc.* **1991**, *113*, 4917−4925.
(41) Desiraju, G. R. Hydrogen Bridges in Crystal Engineering: Interactions without Borders. *Acc. Chem. Res.* **2002**, *35*, 565−573.
(42) de Greef, T. F.; Meijer, E. W. Materials Science: Supramolecular Polymers. *Nature* **2008**, *453*, 171−173.
(43) de Greef, T. F. A.; Smulders, M. M.; Wolffs, M.; Schenning, A. P.; Sijbesma, R. P.; Meijer, E. W. Supramolecular Polymerization. *Chem. Rev.* **2009**, *109*, 5687−5754.
(44) Hoshika, S.; Leal, N. A.; Kim, M.-J.; Kim, M.-S.; Karalkar, N. B.; Kim, H.-J.; Bates, A. M.; Watkins, N. E.; SantaLucia, H. A.; Meyer, A. J.; DasGupta, S.; Piccirilli, J. A.; Ellington, A. D.; SantaLucia, J.; Georgiadis, M. M.; Benner, S. A. Hachimoji DNA and RNA: A Genetic System with Eight Building Blocks. *Science* **2019**, *363*, 884−887.
(45) Swart, M.; Fonseca Guerra, C.; Bickelhaupt, F. M. Hydrogen Bonds of RNA Are Stronger Than Those of DNA, But NMR Monitors Only Presence of Methyl Substituent in Uracil/Thymine. *J. Am. Chem. Soc.* **2004**, *126*, 16718−16719.
(46) Kyogoku, Y.; Lord, R. C.; Rich, A. The Effect of Substituents on the Hydrogen Bonding of Adenine and Uracil Derivatives. *Proc. Natl. Acad. Sci. U. S. A.* **1967**, *57*, 250−257.
(47) Jorgensen, W. L.; Pranata, J. Importance of Secondary Interactions in Triply hydrogen-bonded Complexes: Guanine-Cytosine vs Uracil-2,6-Diaminopyridine. *J. Am. Chem. Soc.* **1990**, *112*, 2008−2010.
(48) Jorgensen, W. L.; Severance, D. L. Chemical Chameleons: Hydrogen Bonding with Imides and Lactams in Chloroform. *J. Am. Chem. Soc.* **1991**, *113*, 209−216.
(49) Murray, T. J. New Triply hydrogen-bonded Complexes with Highly Variable Stabilities. *J. Am. Chem. Soc.* **1992**, *114*, 4010−4011.
(50) Djurdjevic, S.; Leigh, D. A.; McNab, H.; Parsons, S.; Teobaldi, G.; Zerbetto, F. Extremely Strong and Readily Accessible AAA−DDD Triple Hydrogen Bond Complexes. *J. Am. Chem. Soc.* **2007**, *129*, 476−477.
(51) Blight, B. A.; Camara-Campos, A.; Djurdjevic, S.; Kaller, M.; Leigh, D. A.; McMillan, F. M.; McNab, H.; Slawin, A. M. Z. AAA−DDD Triple Hydrogen Bond Complexes. *J. Am. Chem. Soc.* **2009**, *131*, 14116−14122.
(52) Brammer, S.; Lüning, U.; Kühl, C. A New Quadruply Bound Heterodimer DDAD·AADA and Investigations into the Association Process. *Eur. J. Org. Chem.* **2002**, *2002*, 4054−4062.
(53) Beijer, F. H.; Kooijman, H.; Spek, A. L.; Sijbesma, R. P.; Meijer, E. W. Self-Complementarity Achieved through Quadruple Hydrogen Bonding. *Angew. Chem., Int. Ed.* **1998**, *37*, 75−78.
(54) Blight, B. A.; Hunter, C. A.; Leigh, D. A.; McNab, H.; Thomson, P. I. T. An AAAA−DDDD Quadruple Hydrogen-Bond Array. *Nat. Chem.* **2011**, *3*, 244.
(55) Murray, T. J.; Zimmerman, S. C. New Triply hydrogen-bonded Complexes with Highly Variable Stabilities. *J. Am. Chem. Soc.* **1992**, *114*, 4010−4011.
(56) Papmeyer, M.; Vuilleumier, C. A.; Pavan, G. M.; Zhurov, K. O.; Severin, K. Molecularly Defined Nanostructures Based on a Novel AAA−DDD Triple Hydrogen-Bonding Motif. *Angew. Chem.* **2016**, *128*, 1717−1721.
(57) Wilson, A. J. Hydrogen bonding: Attractive arrays. *Nat. Chem.* **2011**, *3*, 193.
(58) Gale, P. A.; Steed, J. W. *Supramolecular Chemistry: From Molecules to Nanomaterials*; Wiley Online Library, 2012; Vol. *8*.
(59) Anslyn, E. V.; Dougherty, D. A. *Modern Physical Organic Chemistry*; University Science Books: Sausalito, CA, 2006.
(60) Tiwari, M. K.; Vanka, K. Exploiting Directional Long Range Secondary Forces for Regulating Electrostatics-Dominated Non-covalent Interactions. *Chem. Sci.* **2017**, *8*, 1378−1390.
(61) Wu, C.-H.; Zhang, Y.; van Rickley, K.; Wu, J. I. Aromaticity Gain Increases the Inherent Association Strengths of Multipoint Hydrogen-Bonded Arrays. *Chem. Commun.* **2018**, *54*, 3512−3515.

DOI: 10.1021/acs.joc.9b02381
J. Org. Chem. 2019, 84, 14805−14815

(62) Lukin, O.; Leszczynski, J. Rationalizing the Strength of Hydrogen-Bonded Complexes. Ab Initio HF and DFT Studies. *J. Phys. Chem. A* **2002**, *106*, 6775−6782.
(63) Popelier, P. L. A.; Joubert, L. The Elusive Atomic Rationale for DNA Base Pair Stability. *J. Am. Chem. Soc.* **2002**, *124*, 8725−8729.
(64) Beijer, F. H.; Sijbesma, R. P.; Kooijman, H.; Spek, A. L.; Meijer, E. W. Strong Dimerization of Ureidopyrimidones via Quadruple Hydrogen Bonding. *J. Am. Chem. Soc.* **1998**, *120*, 6761−6769.
(65) Lin, X.; Jiang, X.; Wu, W.; Mo, Y. Induction, Resonance and Secondary Electrostatic Interaction on Hydrogen Bonding in the Association of Amides and Imides. *J. Org. Chem.* **2018**, *83*, 13446−13453.
(66) Vallejo Narváez, W. E.; Jiménez, E. I.; Cantú-Reyes, M.; Yatsimirsky, A. K.; Hernández-Rodríguez, M.; Rocha-Rinza, T. Stability of Doubly and Triply H-Bonded Complexes Governed by Acidity-Basicity Relationships. *Chem. Commun.* **2019**, *55*, 1556−1559.
(67) Vallejo Narváez, W. E.; Jiménez, E. I.; Romero-Montalvo, E.; Sauza-de la Vega, A.; Quiroz-García, B.; Hernández-Rodríguez, M.; Rocha-Rinza, T. Acidity and Basicity Interplay in Amide and Imide Self-Association. *Chem. Sci.* **2018**, *9*, 4402−4413.
(68) van der Lubbe, S. C. C.; Zaccaria, F.; Sun, X.; Guerra, C. F. Secondary Electrostatic Interaction Model Revised: Prediction Comes Mainly from Measuring Charge Accumulation in Hydrogen-Bonded Monomers. *J. Am. Chem. Soc.* **2019**, *141*, 4878−4885.
(69) Beck, J. F.; Mo, Y. How Resonance Assists Hydrogen Bonding Interactions: An Energy Decomposition Analysis. *J. Comput. Chem.* **2007**, *28*, 455−466.
(70) Šponer, J.; Leszczynski, J.; Hobza, P. Electronic Properties, Hydrogen Bonding, Stacking, and Cation Binding of DNA and RNA Bases. *Biopolymers* **2001**, *61*, 3−31.
(71) Gilli, P.; Bertolasi, V.; Ferretti, V.; Gilli, G. Evidence for Resonance-Assisted Hydrogen Bonding. 4. Covalent Nature of the Strong Homonuclear Hydrogen Bond. Study of the O-H−O System by Crystal Structure Correlation Methods. *J. Am. Chem. Soc.* **1994**, *116*, 909−915.
(72) Gilli, P.; Bertolasi, V.; Ferretti, V.; Gilli, G. Evidence for Intramolecular N-H···O Resonance-Assisted Hydrogen Bonding in b-Enaminones and Related Heterodienes. A Combined Crystal-Structural, IR and NMR Spectroscopic, and Quantum-Mechanical Investigation. *J. Am. Chem. Soc.* **2000**, *122*, 10405−10417.
(73) Gilli, P.; Bertolasi, V.; Pretto, L.; Ferretti, V.; Gilli, G. Covalent versus Electrostatic Nature of the Strong Hydrogen Bond: Discrimination Among Single, Double, and Asymmetric Single-Well Hydrogen Bonds by Variable-Temperature X-Ray Crystallographic Methods in b-Diketone Enol RAHB Systems. *J. Am. Chem. Soc.* **2004**, *126*, 3845−3855.
(74) Gilli, P.; Bertolasi, V.; Pretto, L.; Lyčka, A.; Gilli, G. The Nature of Solid-State N-H···O/O-H···N Tautomeric Competition in Resonant Systems. Intramolecular Proton Transfer in Low-Barrier Hydrogen Bonds Formed by the ···O═C-C═N-NH··· ···HO-C═C-N═N··· Ketohydrazone-Azoenol System. A Variable-Temperature X-Ray Crystallographic and DFT Computational Study. *J. Am. Chem. Soc.* **2002**, *124*, 13554−13567.
(75) Shirota, H.; Ushiyama, H. Hydrogen-Bonding Dynamics in Aqueous Solutions of Amides and Acids: Monomer, Dimer, Trimer, and Polymer. *J. Phys. Chem. B* **2008**, *112*, 13542−13551.
(76) Jeong, K. S.; Tjivikua, T.; Rebek, J. Relative Hydrogen Bonding Affinities of Imides and Lactams. *J. Am. Chem. Soc.* **1990**, *112*, 3215−3217.
(77) Papamokos, G. V.; Demetropoulos, I. N. Vibrational Frequencies of Amides and Amide Dimers: The Assessment of PW91XC Functional. *J. Phys. Chem. A* **2004**, *108*, 7291−7300.
(78) Fonseca Guerra, C.; Zijlstra, H.; Paragi, G.; Bickelhaupt, F. M. Telomere Structure and Stability: Covalency in Hydrogen Bonds, Not Resonance Assistance, Causes Cooperativity in Guanine Quartets. *Chem. - Eur. J.* **2011**, *17*, 12612−12622.
(79) Gilli, G.; Gilli, P. Towards An Unified Hydrogen-Bond Theory. *J. Mol. Struct.* **2000**, *552*, 1−15.
(80) Jiang, X.; Zhang, H.; Wu, W.; Mo, Y. A Critical Check for the Role of Resonance in Intramolecular Hydrogen Bonding (IMHB). *Chem. - Eur. J.* **2017**, *23*, 16885−16891.
(81) Lin, X.; Zhang, H.; Jiang, X.; Wu, W.; Mo, Y. The Origin of the Non-Additivity in Resonance-Assisted Hydrogen Bond (RAHB) Systems. *J. Phys. Chem. A* **2017**, *121*, 8535−8541.
(82) Guevara-Vela, J. M.; Romero-Montalvo, E.; Del Río-Lima, A.; Martín Pendás, Á.; Hernández-Rodríguez, M.; Rocha-Rinza, T. H-Bond Weakening Through p Systems: Resonance-Impaired Hydrogen Bonds (RIHB). *Chem. - Eur. J.* **2017**, *23*, 16605−16611.
(83) Lin, X.; Wu, W.; Mo, Y. A Direct Proof of the Resonance-Impaired Hydrogen Bond (RIHB) Concept. *Chem. - Eur. J.* **2018**, *24*, 1053−1056.
(84) Masumian, E.; Nowroozi, A. Computational Investigation on the Intramolecular Resonance-Inhibited Hydrogen Bonding: A New Type of Interaction versus the RAHB Model. *Theor. Chem. Acc.* **2015**, *134*, 82.
(85) Mo, Y.; Peyerimhoff, S. D. Theoretical Analysis of Electronic Delocalization. *J. Chem. Phys.* **1998**, *109*, 1687−1697.
(86) Mo, Y.; Song, L.; Lin, Y. The Block-Localized Wavefunction (BLW) Method at the Density Functional Theory (DFT) Level. *J. Phys. Chem. A* **2007**, *111*, 8291−8301.
(87) Pauling, L. C. *The Nature of the Chemical Bond*, 3rd ed.; Cornell University Press: Ithaca, NY, 1960.
(88) *Valence Bond Theory*, Cooper, D. L., Ed.; Elsevier: Amsterdam, 2002.
(89) Shaik, S. S.; Hiberty, P. C. *A chemist's guide to valence bond theory*; John Wiley & Sons, 2007.
(90) Wu, W.; Su, P.; Shaik, S.; Hiberty, P. C. Classical Valence Bond Approach by Modern Methods. *Chem. Rev.* **2011**, *111*, 7557−7593.
(91) Gallup, G. A. *Valence Bond Methods: Theory and Applications*; Cambridge University Press: New York, 2002.
(92) Morokuma, K. Why Do Molecules Interact? The Origin of Electron Donor-Acceptor Complexes, Hydrogen Bonding and Proton Affinity. *Acc. Chem. Res.* **1977**, *10*, 294−300.
(93) Chen, W.; Gordon, M. S. Energy Decomposition Analyses for Many-Body Interaction and Applications to Water Complexes. *J. Phys. Chem.* **1996**, *100*, 14316−14328.
(94) Ziegler, T.; Rauk, A. On the Calculation of Bonding Energies by the Hartree Fock Slater Method. *Theor. Chem. Acc.* **1977**, *46*, 1−10.
(95) Mitoraj, M.; Michalak, A.; Ziegler, T. A Combined Charge and Energy Decomposition Scheme for Bond Analysis. *J. Chem. Theory Comput.* **2009**, *5*, 962−975.
(96) Jeziorski, B.; Moszynski, R.; Szalewicz, K. Perturbation Theory Approach to Intermolecular Potential Energy Surfaces of van der Waals Complexes. *Chem. Rev.* **1994**, *94*, 1887−1930.
(97) Andrés, J.; Ayers, P. W.; Boto, R. A.; Carbó-Dorca, R.; Chermette, H.; Cioslowski, J.; Contreras-García, J.; Cooper, D. L.; Frenking, G.; Gatti, C.; Heidar-Zadeh, F.; Joubert, L.; Martín Pendás, Á.; Matito, E.; Mayer, I.; Misquitta, A. J.; Mo, Y.; Pilmé, J.; Popelier, P. L. A.; Rahm, M.; Ramos-Cordoba, E.; Salvador, P.; Schwarz, W. H. E.; Shahbazian, S.; Silvi, B.; Solà, M.; Szalewicz, K.; Tognetti, V.; Weinhold, F.; Zins, É.-L. Nine Questions on Energy Decomposition Analysis. *J. Comput. Chem.* **2019**, *40*, 2248−2283.
(98) Mo, Y.; Bao, P.; Gao, J. Intermolecular Interaction Energy Decomposition Based on Block-Localized Wavefunction and Block-Localized Density Functional Theory. *Phys. Chem. Chem. Phys.* **2011**, *13*, 6760−6775.
(99) Boys, S. F.; Bernardi, F. The Calculation of Small Molecular Interactions by the Differences of Separate Total Energies. Some Procedures with Reduced Errors. *Mol. Phys.* **1970**, *19*, 553−566.
(100) Grimme, S.; Antony, J.; Ehrlich, S.; Krieg, H. A Consistent and Accurate ab Initio Parametrization of Density Functional Dispersion Correction (DFT-D) for the 94 Elements H-Pu. *J. Chem. Phys.* **2010**, *132*, 154104.
(101) Grimme, S.; Mück-Lichtenfeld, C.; Erker, G.; Kehr, G.; Wang, H.; Beckers, H.; Willner, H. When Do Interacting Atoms Form a Chemical Bond? Spectroscopic Measurements and Theoretical

DOI: 10.1021/acs.joc.9b02381
J. Org. Chem. 2019, 84, 14805−14815

Analyses of Dideuteriophenanthrene. *Angew. Chem., Int. Ed.* **2009**, *48*, 2592−2595.
(102) Zhao, Y.; Truhlar, D. G. The M06 Suite of Density Functionals for Main Group Thermochemistry, Thermochemical Kinetics, Noncovalent Interactions, Excited States, and Transition Elements: Two New Functionals and Systematic Testing of Four M06-class Functionals and 12 Other Functionals. *Theor. Chem. Acc.* **2008**, *120*, 215−241.
(103) Hohenstein, E. G.; Chill, S. T.; Sherrill, C. D. Assessment of the Performance of the M05-2X and M06-2X Exchange-Correlation Functionals for Noncovalent Interactions in Biomolecules. *J. Chem. Theory Comput.* **2008**, *4*, 1996−2000.
(104) Thanthiriwatte, K. S.; Hohenstein, E. G.; Burns, L. A.; Sherrill, C. D. Assessment of the Performance of DFT and DFT-D Methods for Describing Distance Dependence of Hydrogen-Bonded Interactions. *J. Chem. Theory Comput.* **2011**, *7*, 88−96.
(105) Walker, M.; Harvey, A. J. A.; Sen, A.; Dessent, C. E. H. Performance of M06, M06-2X, and M06-HF Density Functionals for Conformationally Flexible Anionic Clusters: M06 Functionals Perform Better Than B3LYP for a Model System with Dispersion and Ionic Hydrogen-Bonding Interactions. *J. Phys. Chem. A* **2013**, *117*, 12590−12600.
(106) Schmidt, M. W.; Baldridge, K. K.; Boatz, J. A.; Elbert, S. T.; Gordon, M. S.; Jensen, J. J.; Koseki, S.; Matsunaga, N.; Nguyen, K. A.; Su, S.; Windus, T. L.; Dupuis, M.; Montgomery, J. A. J. General Atomic and Molecular Electronic Structure System. *J. Comput. Chem.* **1993**, *14*, 1347−1363.
(107) Góra, R. W.; Grabowski, S. J.; Leszczynski, J. Dimers of Formic Acid, Acetic Acid, Formamide and Pyrrole-2-Carboxylic acid: An Ab Initio Study. *J. Phys. Chem. A* **2005**, *109*, 6397−6405.
(108) Lopes Jesus, A. J.; Redinha, J. S. Charge-Assisted Intramolecular Hydrogen Bonds in Disubstituted Cyclohexane Derivatives. *J. Phys. Chem. A* **2011**, *115*, 14069−14077.

DOI: 10.1021/acs.joc.9b02381
J. Org. Chem. 2019, 84, 14805−14815